YMTHE, Volume *30*

Supplemental Information

Ectopic clotting factor VIII expression and misfolding in hepatocytes as a cause for hepatocellular carcinoma

Audrey Kapelanski-Lamoureux, Zhouji Chen, Zu-Hua Gao, Ruishu Deng, Anthoula Lazaris, Cynthia Lebeaupin, Lisa Giles, Jyoti Malhotra, Jing Yong, Chenhui Zou, Ype P. de Jong, Peter Metrakos, Roland W. Herzog, and Randal J. Kaufman

SUPPLEMENTAL MATERIALS

Materials and Methods

Materials for cellular and molecular biology

Anti-factor VIII heavy chain monoclonal antibody coupled to Sepharose CL-4B was a kind gift from Baxter/Baxalta Corp. FVIII-deficient and normal pooled human plasmas were obtained from George King Biomedical (Overland Park, KS). Activated partial thromboplastin (automated aPTT reagent) and $CaCl_2$ were purchased from General Diagnostics Organon Teknika (Durham, NC). Dulbecco's modified Eagle medium (DMEM), glucose-free DMEM, alpha-modified essential medium (alpha-MEM), cysteine/methionine-free DMEM, and fetal bovine serum (FBS) were purchased from Gibco BRL. FVIII:C-EIA was purchased from Affinity Biologicals. Anti-β-actin antibody, 3-methyladenine, 2-deoxy-D-glucose (2-DG), and sodium azide (NaN_3) were obtained from Sigma Aldrich. Anti-FVIII antibody (GMA012) was obtained from Green Mountain. [^{35}S]-Methionine/Cysteine was obtained from MP Biologicals. Mouse and rabbit horseradish peroxidase conjugated secondary antibodies, Prolong Antifade Gold and Complete Protease Inhibitor Cocktail were obtained from Promega. Supersignal West Pico ECL was obtained from Thermo. Mouse FAB fragments, Dylight 549 conjugated anti-mouse fab fragments and Texas-Red conjugated anti-mouse secondary were obtained from Jackson Immunoresearch (West grove, PA).

Mice

Male *C57BL/6J* mice were purchased from Jackson Laboratory and maintained at the Sanford-Burnham-Prebys Medical Discovery Institute animal facility. Mice were euthanized by CO_2 inhalation for liver harvest. All animal protocols were reviewed and approved by the Institutional Animal Care and Use Committee at the SBP Medical Discovery Institute.

Hydrodynamic tail vein injection of plasmid DNA and HCC development

The expression vectors for BDD and N6 were previously described.[1] Six wk-old male mice were used for these experiments. Hydrodynamic tail vein DNA injection was performed according to previous publications.[2,3] In summary, 100μg plasmid DNA was diluted in 2.5ml saline and injected into mice through the tail vein. One wk after the injection, mice were fed 60% HFD for 65 wks after which their livers were harvested for tumor evaluation.

Glucose depletion and repletion

For glucose depletion, cells were treated with ATP-depleting medium (glucose-free DMEM containing 20 mM 2-DG and 10 mM NaN_3) for 2 hr. To replete glucose, fresh media was replaced for the indicated time. Cycloheximide (CHX) at a final concentration of 10 μg/mL was added to the repletion media where indicated.

Factor VIII activity and antigen analysis

FVIII activity was measured by a 1-stage activated thromboplastin time (aPTT) clotting assay on an MLA Electra 750 fibrinometer (Medical Laboratory Automation, Pleasantville, NY) by reconstitution of human FVIII-deficient plasma. The FVIII plasma standard was FACT plasma (normal pooled plasma) from George King Biomedical. FVIII antigen was quantified by an anti-FVIII sandwich enzyme-linked immunosorbent assay (ELISA) method using the Affinity Biologicals FVIII:C-EIA commercial kit (Affinity Biologicals Inc., Hamilton, ON, Canada) according to the manufacturers' instructions.

Metabolic labeling

Cells were subcultured 24 hr prior to labeling in 60 mm dishes (approximately 10^6 cells/plate) and were 80% confluent at the time of labeling. Cells were washed twice in cys/met free DMEM and incubated in cys/met-free DMEM for 10 min prior to labeling. Cells were labeled in 0.5 ml Cys/Met free DMEM containing 100 μCi/mL (BDD-FVIII and N6-FVIII) for 20 min and chased for the indicated times with conditioned medium (either 2-DG and NaN_3-containing medium or normal medium) containing excess unlabeled Cys and Met and 10 μg/ml aprotinin. For glucose-depletion/repletion conditions, depleting medium was removed after 2 hr and replaced with normal medium containing excess unlabeled Cys and Met and aprotinin as above. At the end of the chase period, conditioned media was collected. Cells were rinsed three times in phosphate buffered saline (PBS) and harvested in 1 ml lysis buffer [50 mM Tris-HCl, pH 7.4, 150 mM NaCl, 0.1% (v/v) Triton X-100, and 1% (v/v) IGEPAL] containing Complete Protease Inhibitor Cocktail and 1 mM phenylmethylsulfonyl fluoride. Lysates were incubated on ice 30 min, followed by centrifugation at 15,000 x g for 10 min. Post-nuclear supernatant was then assayed for protein content using BCA assay (Bio-Rad). Equal amounts of protein and corresponding amounts of media were subjected to FVIII immunoprecipitation (IP) using anti-FVIII coupled Sepharose CL-4B beads at 4˚C overnight. IPs were washed 4 times with lysis buffer and proteins were separated by reducing SDS-PAGE. IP'd proteins were visualized by autoradiography and band intensities were quantified using ImageQuant normal media for indicated times. CHX at a final concentration of 10 μg/mL was added to the repletion media where indicated.

Interaction of BDD and N6 with BiP *in vivo.*

The *BiP-Flag* mice were generated as described.[4] Mice were fed a regular mouse chow diet. Induction of BiP-Flag expression was initiated at the age of 6 wks by transduction with AAV8-TGB-Cre.[4] AAV8-TGB-Cre-transdcued wild type littermates were used as controls. At 6 wks after AAV8-TGB-Cre-transduction, the mice received the parental pMT2 vector, BDD vector, or N6 vector as detailed in Figure 3 through hydrodynamic tail vein DNA injection[3] and were sacrificed to collect liver tissues 26 hr post-vector DNA injection.

Liver samples were harvested in lysis buffer [0.15 mM NaCl, 0.5% Triton X-100, 20 mM HEPES, pH 7.4, 1x Protease inhibitor cocktail (Fisher)]. The liver lysates were centrifuged at 10K x g for 10 min and the resultant supernatants were used for subsequent analyses. For anti-Flag IP, 120 μg of lysate proteins in 300 μl of lysis buffer was mixed with 15 μl of M2 anti-Flag magnetic beads (Sigma) and incubated with rotation at 4°C for 4 hr.

At the end of this incubation, the anti-Flag beads were washed 3X with ice-cold lysis buffer (1 ml each). Proteins in the washed anti-Flag and anti-FVIII beads were eluted with SDS-PAGE loading buffer, separated by SDS-PAGE under reducing conditions and transferred onto Nitrocellulose membranes for Western blotting along with 32 μg proteins for each liver lysate sample used for Flag IP (ie., 25% of the input). A mouse anti-human FVIII monoclonal antibody (GAM012, Santa Cruz Biotechnology) was used for BDD and N6 detection.

***Ex vivo* studies with mouse-passaged primary human hepatocytes**

Mouse-passed primary human hepatocytes (PHH) were prepared and cultured as described.[5] They were transduced with a lentiviral vector expressing a codon-optimized form of SQ-BDD coding sequence (Lenti-BDD)[6] at the indicated doses 3 days after isolation and being cultured *ex vivo* and harvested for Western blot analysis 10 days after transduction.

Antibodies used were as follows: Rabbit anti-BiP, rabbit anti-phospho eIF2α and rabbit anti- eIF2α were from Cell Signaling Technology, (Danvers, MA). Mouse anti-human FVIII was from Green Mountain Antibodies (Burlington, VT); Rabbit anti-CRELD2 and mouse anti-hepcidin antibodies were from Proteintech (Rosemont, IL) and Novus Biologicals (Burlington, Vt), respectively. Mouse anti-beta actin was from ThermoFisher (Waltham, MA).

Time-course study of BDD and N6 expression after DNA vector delivery

Male *C57BL/6J* mice (6-8 weeks old) received pMT, pMT-BDD, or pMT-N6 vector DNA through hydrodynamic tail vein injection described above. Plasma samples were collected at 23-24 h after DNA vector injection via orbital vein bleeding. Mice were sacrificed either at 24 h or 7 days after vector DNA injection to harvest liver and plasma samples. Sodium citrate (final concentration= 0.4%) was used as an anticoagulant for all blood samples. BDD and N6 levels in the plasma samples and liver homogenates were determined using a human FVIII-specific ELISA kit (Affinity Biologicals Inc.). Hepatic levels of BDD and N6 transcripts were measured by quantitative RT-PCR (RT-qPCR) as described[7] using the following PCR primer pairs for mouse beta-actin (*Actb*) and human F8 (F8), respectively: *Actb*-fw 5'-GGCTGTATTCCCCTCCATCG-3', *Actb*-rev 5'-CCAGTTGGTAACAATGCCATGT-3'; F8-fw 5'-GCATTCGCAGCACTCTTCG-3', F8-rev 5'-GAGGTGAAGTCGAGCTTTTGAA-3'. The RNA samples were subjected to DNAse-treatment using a Turbo DNA-free kit (Fisher Scientific, Waltham, MA) to eliminate contamination with pMT-BDD and pMT-N6 vectors before being used for RT-qPCR analysis.

Histology and immunohistochemistry staining

Formalin-fixed paraffin-embedded (FFPE) blocks of mouse livers were prepared from empty vector, BDD, and N6-transduced mice. Tissue fixation and paraffin embedding was performed following routine methods. Four μm-thick serial sections were cut from each FFPE block and adhered to charged glass slides (Superfrost Plus; Fisher Scientific, Waltham, MA, USA). Sections were incubated at 60°C for 1 hr prior to deparaffinization in xylene and then rehydrated in 100%, 95%, and double-distilled water successively. Sections were heat-induced in retrieval

buffer at pH 6.0, incubated with peroxidase block (Dako, Mississauga, ON, Canada) for 20 min followed by blocking (5% goat serum in 1% PBS-T) for 1 hr. Sections were then incubated overnight at 4°C with primary antibodies diluted in blocking buffer. Primary antibodies used for this study were: rabbit anti-GS (Glutamine Synthetase: Abcam, Cambridge, UK, ab176562; dilution 1:1000), rabbit anti-CD34 (Abcam, Cambridge, UK, ab81289; dilution 1:2500), rabbit anti-CTNNB1 (β-catenin: Abcam, Cambridge, UK, ab223075; dilution 1:4800), rabbit anti-CD44 (Abcam, Cambridge, UK, ab157107; dilution 1:2500), rabbit anti-GPC3 (Glypican-3: LSBio, Seattle, USA, LS-B13373; dilution 1:4000), rabbit anti-BiP (Binding Immunoglobulin Protein: Cell Signaling Technology, Massachusetts, USA, #3177; dilution 1:600). The detection system used was the EnVision+ System-HRP kit (Dako, K4007). Sections were counterstained with hematoxylin prior to dehydration and mounted with Permount (Fisher, SP-15-100). The first section of each series was stained with Hematoxylin and Eosin (H&E) and the fifth section was stained with reticulin (Abcam, #ab150684) for an initial histopathological assessment. Immunohistochemistry with Thio-S and FVIII antibodies was performed as described.[8]

Scoring analysis

Slides were scanned using the Aperio AT Turbo system at 20x magnification and viewed using the Aperio Image Scope system. The positivity [Total number of positive pixels divided by total number of pixels: (NTotal – Nn)/(NTotal)] was assessed using the positive pixel count algorithm from the ImageScope software (positive pixel count V9, Aperio, Inc.). The algorithm outputs a strong, moderate, and weak intensity range. The total signal positivity was used to quantify all immunohistochemistry markers where only the strong signal positivity was used as a measure of total positivity of apoptotic cells for TUNEL assay positivity quantification. Signal positivity was analyzed at the central tumor, the interface and distal normal liver.

Histopathological analysis

All slides were analyzed, in a blinded fashion, by a board-certified pathologist who evaluated the presence of hepatocellular adenomas and carcinomas based on an immunohistology analysis and various morphometrical features unique to each type.

The following are the stains used to first confirm the lesions and to evaluate whether they represent adenomas (benign disease) or carcinomas. Reticulin staining is intended to demonstrate reticular fibers surrounding tumor cells. Tumors that retain a reticulin network are generally benign or pre-neoplastic, whereas HCC loses the reticulin fiber normal architecture.[9,10] CD34 is a marker of “capillarization”, a process by which sinusoid endothelial cells lose their fenestration. CD34 demonstrates neovascularization in HCC, while nontumorous hepatic sinusoids do not stain with CD34.[10-12] However, it was previously reported that in some cases, CD34 may occur diffusely or in areas of hepatocellular adenoma.[9] Glypican 3 (GPC3) was identified as a tumor marker for the diagnosis of HCC due to its specificity and sensitivity.[10,13-15] GPC3 shows a cytoplasmic, membranous and canalicular staining among HCCs. However, among livers with a cirrhotic background, GPC3 expression can also be found focally. Although GPC3 is a specific immunomarker for HCC, and show negative staining in

adenomas, the diagnosis of HCC should not only rely on this marker.[16,17] Glutamine synthetase (GS) stains positively for zone 3 of the liver parenchyma. GS overexpression is related to a β-catenin mutation which is a well-known indicator for malignant transformation.[18] Most HCCs show strong positive cytoplasmic staining while adenomas are known to stain for GS at variable frequencies[14,19,20]. Consequently, GS is a less valuable immunomarker for differentiating HCC from adenomas and alternatively preferred to differentiate between HCC and dysplastic nodules. Beta-catenin shows membranous positive staining on normal hepatocytes. Activation of β-catenin leads to cytoplasmic and nuclear accumulation of β-catenin, which is suggestive of malignant transformation.[21,22] Finally, CD44 is an adhesion molecule found on sinusoidal lymphocytes and Kupffer cell types in normal liver.[23-25] Expression of CD44 in HCC cells has been associated with invasive properties.[26]

Apart from the above immunohistology analysis, the lesions categorization into hepatocellular adenoma or hepatocellular carcinoma was further supported based on the identification of 4 morphometrical features. Hepatocellular adenoma was defined as 1. hepatocellular plates 1-2 cells thick 2. nuclear density (#nuclei/mm^2) <1.5x of adjacent non-neoplastic liver, 3. no obvious nuclear atypia, 4. no pseudogland formation. Hepatocellular carcinoma defined as 1. hepatocellular plates >3 cells thick, 2. nuclear density > or =1.5X of adjacent non-neoplastic liver, 3. obvious nuclear atypia, 4. presence of occasional pseudoglands.[27]

Microdissection and DNA analysis of the tumor and non-tumor tissues

Manual microdissection was used to isolate specific regions from FFPE BDD and N6 normal liver and tumor tissue samples. Sectioning was performed by cutting 7 µm thick sections of the FFPE tissue samples using the microtome and sections are mounted on charged glass slides (Superfrost Plus; Fisher Scientific, Waltham, MA, USA). Regions of interest were selected by visually using an inverted light microscope and tissues were manually scraped into 1.5-ml microcentrifuge tubes. Between 6 to 10 tissue sections were collected into each tube and stored at -20ºC prior to DNA isolation. FFPE liver blocks prepared from saline- and pMT-BDD-injected mice that were sacrificed at 24 h after hydrodynamic tail vein injection were used as negative and positive controls, respectively, for this experiment. DNA were isolated from the dissected tissues using a QIAamp DNA FFPE Tissue Kit (Qiagen Inc., Valencia, CA) according to the manufacturer's instruction. Approximately ~0.2 µg DNA from each sample was used for direct qPCR analysis to detect BDD and N6 coding sequences in the tumor and non-tumor tissues using a CFX384 Real-Time System (Bio-Rad, Hercules, CA) described for RT-qPCR.[7] The same primer pair that was used for RT-qPCR analysis of BDD and N6 transcripts described above (i.e, F8-fw 5'-GCATTCGCAGCACTCTTCG-3', F8-fw 5'-GAGGTGAAGTCGAGCTTTTGAA-3') was used for this purpose whereas the following primer pair was used for amplification of mouse beta actin (*Actb*) genomic sequence: *Actb*-genomic-fw: 5'-AACCGTGAAA AGATGACCCAG-3', *Actb*-genomic-rev: 5'-CACAGCCTGGAT GGCTACGTA-3'.

Statistical Analyses

Statistical analyses were performed using GraphPad Prism 9. Chi-square test was used for comparing of tumor incidence between BDD and N6 groups. A p value < 0.05 was regarded as statistically significant. Statistical analysis for immunohistochemistry was performed with a two-tailed Student's *t*-test. *P* values of <0.05 were considered significant ($p < 0.05$ *, $p < 0.01$ **, $p < 0.001$ ***).

References

1. Miao, H.Z., Sirachainan, N., Palmer, L., Kucab, P., Cunningham, M.A., Kaufman, R.J., and Pipe, S.W. (2004). Bioengineering of coagulation factor VIII for improved secretion. Blood *103*, 3412-3419. 10.1182/blood-2003-10-3591.
2. Liu, F., Song, Y., and Liu, D. (1999). Hydrodynamics-based transfection in animals by systemic administration of plasmid DNA. Gene Ther *6*, 1258-1266. 10.1038/sj.gt.3300947.
3. Malhotra, J.D., Miao, H., Zhang, K., Wolfson, A., Pennathur, S., Pipe, S.W., and Kaufman, R.J. (2008). Antioxidants reduce endoplasmic reticulum stress and improve protein secretion. Proc Natl Acad Sci U S A *105*, 18525-18530. 10.1073/pnas.0809677105.
4. Peng, Y., Chen, Z., Jang, I., Arvan, P., and Kaufman, R.J. (2021). Epitope-tagging of the endogenous murine *BiP/GRP78/Hspa5* locus allows direct analysis of the BiP interactome and protein misfolding *in vivo*. bioRxiv, 2020.2001.2001.892539. 10.1101/2020.01.01.892539.
5. Michailidis, E., Vercauteren, K., Mancio-Silva, L., Andrus, L., Jahan, C., Ricardo-Lax, I., Zou, C., Kabbani, M., Park, P., Quirk, C., Pyrgaki, C., et al. (2020). Expansion, in vivo-ex vivo cycling, and genetic manipulation of primary human hepatocytes. Proc Natl Acad Sci U S A *117*, 1678-1688. 10.1073/pnas.1919035117.
6. Ward, N.J., Buckley, S.M., Waddington, S.N., Vandendriessche, T., Chuah, M.K., Nathwani, A.C., McIntosh, J., Tuddenham, E.G., Kinnon, C., Thrasher, A.J., and McVey, J.H. (2011). Codon optimization of human factor VIII cDNAs leads to high-level expression. Blood *117*, 798-807. 10.1182/blood-2010-05-282707.
7. Jang, I., Pottekat, A., Poothong, J., Yong, J., Lagunas-Acosta, J., Charbono, A., Chen, Z., Scheuner, D.L., Liu, M., Itkin-Ansari, P., Arvan, P., et al. (2019). PDIA1/P4HB is required for efficient proinsulin maturation and ss cell health in response to diet induced obesity. Elife *8*. 10.7554/eLife.44528.
8. Poothong, J., Pottekat, A., Siirin, M., Campos, A.R., Paton, A.W., Paton, J.C., Lagunas-Acosta, J., Chen, Z., Swift, M., Volkmann, N., Hanein, D., et al. (2020). Factor VIII exhibits chaperone-dependent and glucose-regulated reversible amyloid formation in the endoplasmic reticulum. Blood *135*, 1899-1911. 10.1182/blood.2019002867.
9. Brunt, E.M. (2012). Histopathologic features of hepatocellular carcinoma. Clin Liver Dis (Hoboken) *1*, 194-199. 10.1002/cld.98.
10. Torbenson, M.S. (2015). Hepatocellular Carcinoma. In Surgical Pathology of Liver Tumors, T. Mounajjed, V.S. Chandan, and M.S. Torbenson, eds. (Cham: Springer International Publishing), pp. 169-218. 10.1007/978-3-319-16089-4_7.
11. Coston, W.M., Loera, S., Lau, S.K., Ishizawa, S., Jiang, Z., Wu, C.L., Yen, Y., Weiss, L.M., and Chu, P.G. (2008). Distinction of hepatocellular carcinoma from benign hepatic mimickers using Glypican-3 and CD34 immunohistochemistry. Am J Surg Pathol *32*, 433-444. 10.1097/PAS.0b013e318158142f.
12. Maeda, T., Adachi, E., Kajiyama, K., Takenaka, K., Honda, H., Sugimachi, K., and Tsuneyoshi, M. (1995). CD34 expression in endothelial cells of small hepatocellular carcinoma: its correlation with tumour progression and angiographic findings. J Gastroenterol Hepatol *10*, 650-654. 10.1111/j.1440-1746.1995.tb01365.x.
13. Wasfy, R.E., and Shams Eldeen, A.A. (2015). Roles of Combined Glypican-3 and Glutamine Synthetase in Differential Diagnosis of Hepatocellular Lesions. Asian Pac J Cancer Prev *16*, 4769-4775. 10.7314/apjcp.2015.16.11.4769.
14. Takahashi, Y., Dungubat, E., Kusano, H., Ganbat, D., Tomita, Y., Odgerel, S., and Fukusato, T. (2021). Application of Immunohistochemistry in the Pathological Diagnosis of Liver Tumors. Int J Mol Sci *22*. 10.3390/ijms22115780.
15. Yan, B., Wei, J.J., Qian, Y.M., Zhao, X.L., Zhang, W.W., Xu, A.M., and Zhang, S.H. (2011). Expression and clinicopathologic significance of glypican 3 in hepatocellular carcinoma. Ann Diagn Pathol *15*, 162-169. 10.1016/j.anndiagpath.2010.10.004.

16. Wang, H.L., Anatelli, F., Zhai, Q.J., Adley, B., Chuang, S.T., and Yang, X.J. (2008). Glypican-3 as a useful diagnostic marker that distinguishes hepatocellular carcinoma from benign hepatocellular mass lesions. Arch Pathol Lab Med *132*, 1723-1728. 10.1043/1543-2165-132.11.1723
10.5858/132.11.1723.
17. Lagana, S.M., Salomao, M., Bao, F., Moreira, R.K., Lefkowitch, J.H., and Remotti, H.E. (2013). Utility of an immunohistochemical panel consisting of glypican-3, heat-shock protein-70, and glutamine synthetase in the distinction of low-grade hepatocellular carcinoma from hepatocellular adenoma. Appl Immunohistochem Mol Morphol *21*, 170-176. 10.1097/PAI.0b013e31825d527f.
18. Bioulac-Sage, P., Rebouissou, S., Thomas, C., Blanc, J.F., Saric, J., Sa Cunha, A., Rullier, A., Cubel, G., Couchy, G., Imbeaud, S., Balabaud, C., et al. (2007). Hepatocellular adenoma subtype classification using molecular markers and immunohistochemistry. Hepatology *46*, 740-748. 10.1002/hep.21743.
19. Lagana, S.M., Moreira, R.K., Remotti, H.E., and Bao, F. (2013). Glutamine synthetase, heat shock protein-70, and glypican-3 in intrahepatic cholangiocarcinoma and tumors metastatic to liver. Appl Immunohistochem Mol Morphol *21*, 254-257. 10.1097/PAI.0b013e3182642c9c.
20. Gebhardt, R., Tanaka, T., and Williams, G.M. (1989). Glutamine synthetase heterogeneous expression as a marker for the cellular lineage of preneoplastic and neoplastic liver populations. Carcinogenesis *10*, 1917-1923. 10.1093/carcin/10.10.1917.
21. Garcia-Buitrago, M.T. (2017). Beta-Catenin Staining of Hepatocellular Adenomas. Gastroenterol Hepatol (N Y) *13*, 740-743.
22. Tien, L.T., Ito, M., Nakao, M., Niino, D., Serik, M., Nakashima, M., Wen, C.Y., Yatsuhashi, H., and Ishibashi, H. (2005). Expression of beta-catenin in hepatocellular carcinoma. World J Gastroenterol *11*, 2398-2401. 10.3748/wjg.v11.i16.2398.
23. Flanagan, B.F., Dalchau, R., Allen, A.K., Daar, A.S., and Fabre, J.W. (1989). Chemical composition and tissue distribution of the human CDw44 glycoprotein. Immunology *67*, 167-175.
24. Picker, L.J., Nakache, M., and Butcher, E.C. (1989). Monoclonal antibodies to human lymphocyte homing receptors define a novel class of adhesion molecules on diverse cell types. J Cell Biol *109*, 927-937. 10.1083/jcb.109.2.927.
25. Volpes, R., Van Den Oord, J.J., and Desmet, V.J. (1992). Vascular adhesion molecules in acute and chronic liver inflammation. Hepatology *15*, 269-275. 10.1002/hep.1840150216.
26. Mathew, J., Hines, J.E., Obafunwa, J.O., Burr, A.W., Toole, K., and Burt, A.D. (1996). CD44 is expressed in hepatocellular carcinomas showing vascular invasion. J Pathol *179*, 74-79. 10.1002/(SICI)1096-9896(199605)179:1<74::AID-PATH531>3.0.CO;2-E.
27. Motohashi, I., Okudaira, M., Takai, T., Kaneko, S., and Ikeda, N. (1992). Morphological differences between hepatocellular carcinoma and hepatocellular carcinomalike lesions. Hepatology *16*, 118-126. 10.1002/hep.1840160120.
28. Washington, K., Telen, M.J., and Gottfried, M.R. (1997). Expression of cell adhesion molecule CD44 in primary tumors of the liver: an immunohistochemical study. Liver *17*, 17-23. 10.1111/j.1600-0676.1997.tb00773.x.
29. Basakran, N.S. (2015). CD44 as a potential diagnostic tumor marker. Saudi Med J *36*, 273-279. 10.15537/smj.2015.3.9622.

Supplemental Data:

Figure S1, Figure S2, Figure S3, Table S1, Table S2, Table S3, and Table S4.

Figure S1

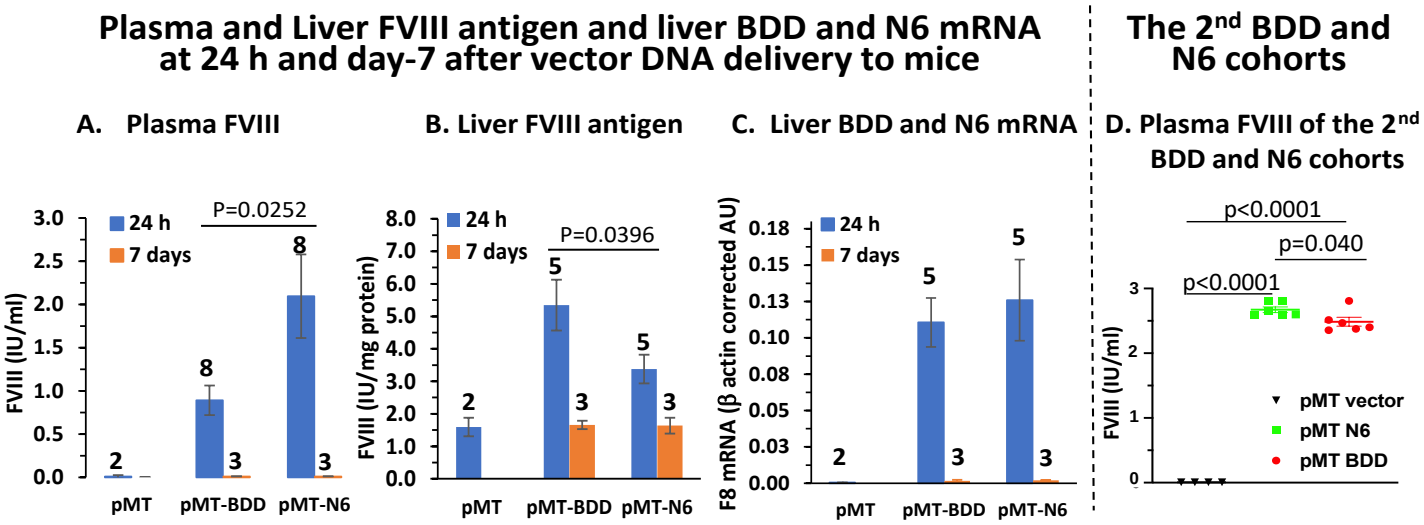

Figure S1. Plasma and Liver FVIII antigen and hepatic BDD and N6 transcripts were undetectable 7 days after vector DNA delivery to mice. A) Plasma BDD and N6 antigen. **B)** Liver human FVIII antigen. **C)** Liver BDD and N6 mRNA levels. Mice were sacrificed at 24 h or 7 days after hydrodynamic tail injection of pMT, pMT-BDD or pMT-N6 DNA vectors. Data are represented as mean ± S.E.M. The numbers on the top of each bar in the graphs of panels A-C are the number of mice (n) for the corresponding data. **D)** Plasma antigen levels of BDD and N6 for the second cohort of TM-BDD and TM-N6 mice that were used for the tumor study described in Figures 6 and S2. Plasma samples from these mice were also obtained at 24 h after vector DNA injection. Plasma BDD and N6 antigen levels in these mice appeared to be higher levels than those shown in Figures 6A. This difference might have resulted from variable nature of the DNA delivery, ELISAs performed at different times, as well as murine housing conditions.

Figure S2

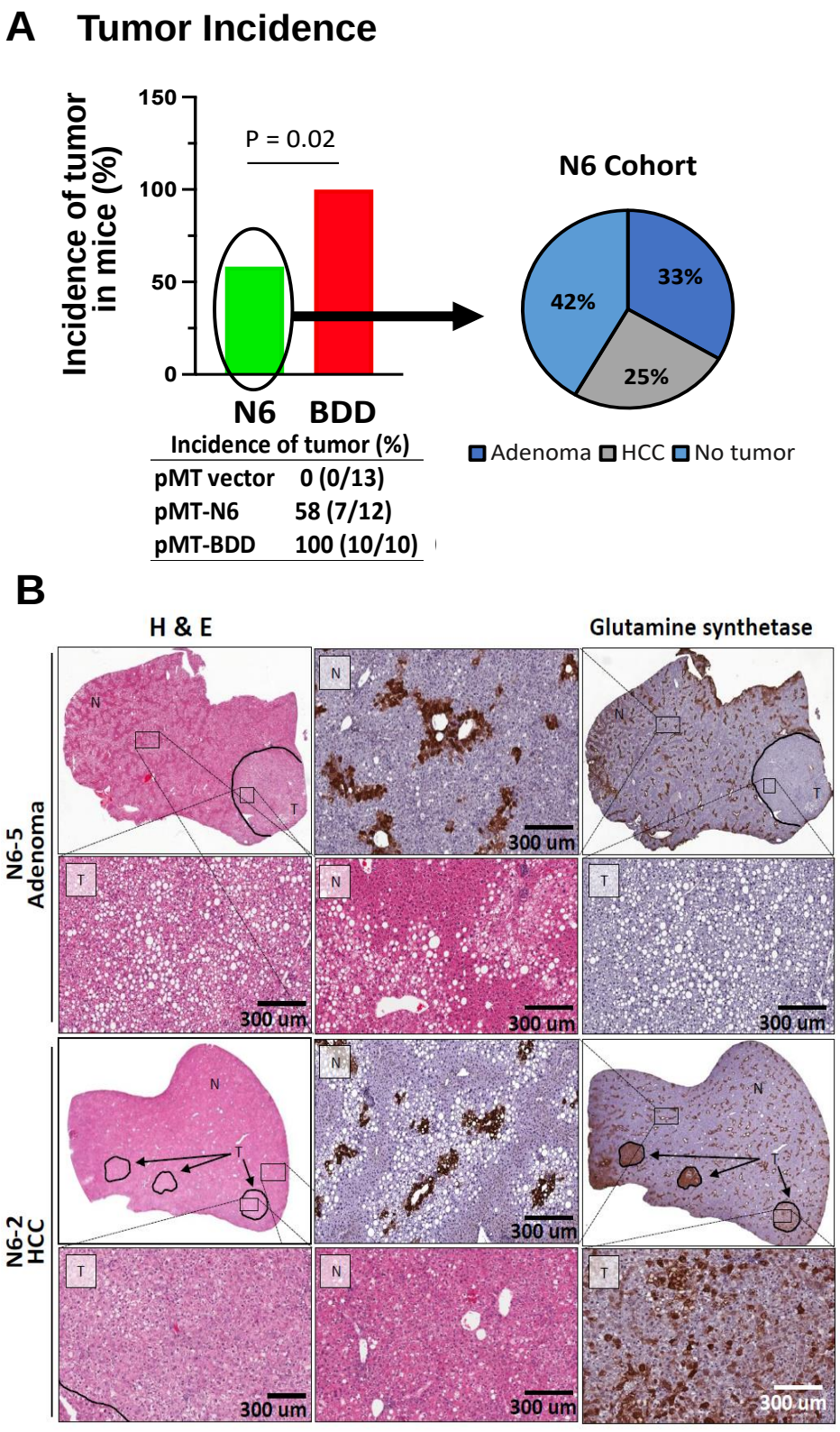

Figure S2. Liver surface tumors in mice injected with N6 vector DNA. Mice were injected with BDD, N6, or empty vector DNA and treated with a high-fat diet as described in Methods and legend to Fig. 6. **A)** Distribution of HCC and adenomas among liver tumors in the N6 cohort. **B)** Positivity for glutamine synthase stains was observed in HCC but not in adenoma of the N6 mice. T=tumor, NT=non-tumor.

Figure 3S

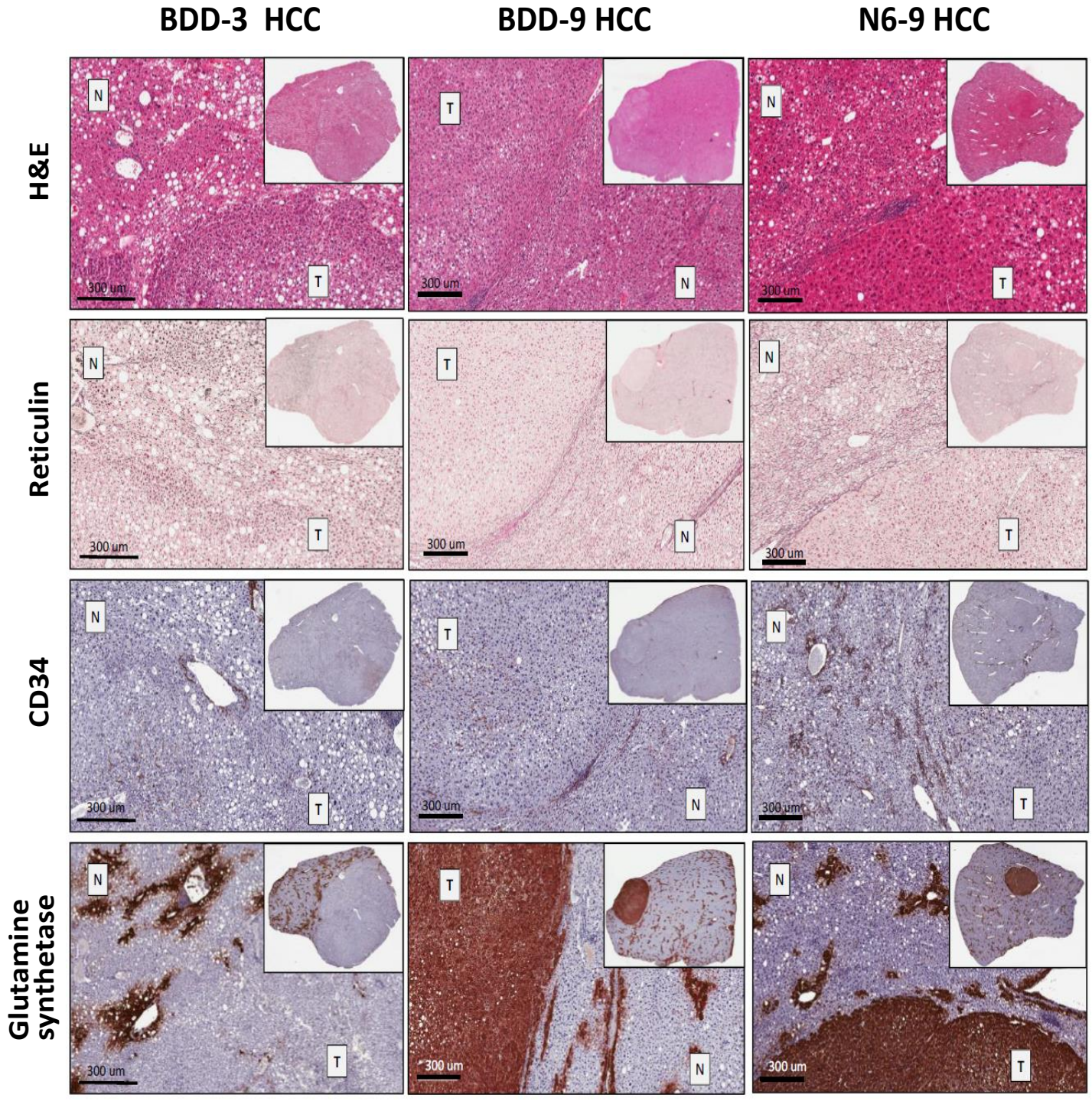

Figure S3. Representative immunohistochemistry characterization of HCC samples. Serial sections were stained for H&E: Hematoxylin and Eosin, reticulin, CD34, glutamine synthetase, glypican-3, β-catenin, and CD44. T=tumor, NT=non-tumor.

Figure 3S (continued)

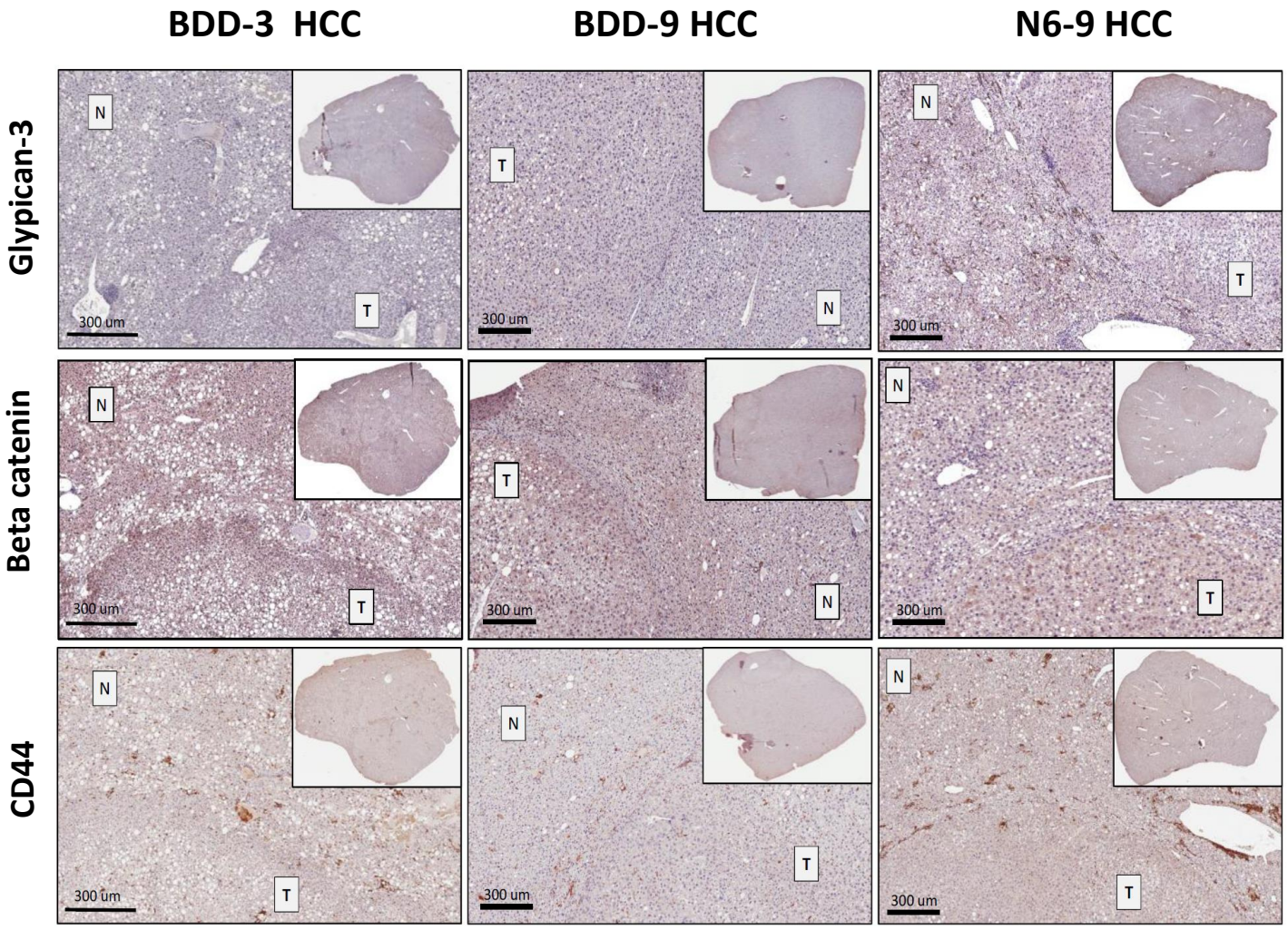

Figure S3 (continued). Representative immunohistochemistry characterization of HCC samples. Serial sections were stained for glypican-3, β-catenin, and CD44. T=tumor, NT=non-tumor.

Table S1. Immunohistochemistry characterization of the pMT- BDD cohort samples.

	H&E	Glutamine synthetase	CD34	Reticulin	B-catenin	CD44	Glypican 3
BDD-10	Steatosis involves about 30% liver parenchyma with mild steatohepatitis. There is one large well-defined lesion with 75% steatosis, inflammation and ductular proliferation favor **liver cell adenoma**. Focal nodular hyperplasia is in the differential.	Tumor completely negative	Patchy strong positive in the center of the lesion	Patchy loss of reticulin network.	Mostly negative (80%) Focal (10%) patchy cytoplasmic and nuclear positivity Other 10% positive cells are inflammatory cells	Some sinusoidal lymphocytes positive, all lesional hepatocytes negative	Lesion negative.
BDD-9	Steatosis involves about 5% liver parenchyma with no steatohepatitis. Occasional portal tract has dense lymphplasmacytic aggregate. A well demarcated nodule with mild cytological atypia, **early HCC.**	The tumor stained completely positive, may indicate malignant	Lesion negative	Tumor nearly completely loss of reticulin network, favor malignant	Lesion negative	Lesion negative	Focal weak positivity (1+) especially in cells showing nuclear atypia
BDD-8	Steatosis involves about 5% liver parenchyma with no steatohepatitis. A tumor lesion with poorly defined borders and cytological atypia, could be an **early HCC.**	Entire slide stained positive, patchy pale focus, may indicate malignant	Lesion mostly negative, at one end, Patchy strong positivity	Reticulin is lost in 80% of the lesion	Nuclear positivity present	Lesion negative	Lesion showed patchy positivity 1+.
BDD-7	Steatosis involves about 55% liver parenchyma with mild steatohepatitis. There is a small poorly demarcated nodule at the center of the slide, favors a **very early evolving HCC**	Very small poorly developed lesion area, stained negative	Lesional area positive, periphery, extend to the center	Lesional area showed diminished reticulin and focal loss.	Lesion negative	Some sinusoidal lymphocytes positive, all lesional and non-lesional hepatocytes negative	Lesion completely negative
BDD-6	Steatosis involves about 5% liver parenchyma with no steatohepatitis. There is a large lesion with significant ballooning, inflammation, nodularity and focal ductular proliferation. Favor **liver cell adenoma** inflammatory subtype.	Lesion negative Favor adenoma, ruled out FNH	Overall, the lesion is negative	Lesion showed diminished reticulin and focal loss.	Lesion negative	Some sinusoidal lymphocytes positive, all lesional and non-lesional hepatocytes negative	Lesion completely negative
BDD-5	Steatosis involves about 30% liver parenchyma with mild steatohepatitis. There is one large well-defined lesion with 100% steatosis, and bland cytology. **Favor liver cell adenoma.** Above that, a small round nodule also present.	Upper small nodule negative. Lesion middle area negative Lesion lower area patchy positive normal liver pattern.	Positive mostly at the periphery of the upper small round nodule. Lower large lesion negative	Upper small nodule completely lost reticulin. Remaining lesion showed diminished reticulin.	Lesion negative	Upper small nodule negative. The larger nodule showed focal hepatocyte 1+ membranous positivity.	Upper small nodule negative. Large nodule mostly negative. At the lower part, focal positivity at the edge with no corresponding HCC morphology
BDD-4	Steatosis involves about 30% liver parenchyma with mild steatohepatitis. There is one large well-defined lesion with 40% steatosis, and bland cytology, **favor liver cell adenoma.**	Lesion negative	Lesion negative	Reticulin present in at least 50% of the lesion. Diminished reticulin network.	Lesion negative	Lesion negative	Lesion negative
BDD-3	Steatosis involves about 45% liver parenchyma with mild steatohepatitis. There is one focus of **well differentiated HCC** arising from a large liver cell adenoma.	Lesion negative	With the nodule, a strong positive area "nodule in nodule) support HCC arising from an adenoma	Approximately 65% of lesion showed loss of reticulin Diminished reticulin network. The area with no reticulin correspond to the malignant looking area in HE	Some cytoplasmic stain see especially in the "HCC" area, no obvious nucleus stain	Some sinusoidal lymphocytes positive, all lesional and non-lesional hepatocytes negative	Lesion negative
BDD-2	Steatosis involves about 5% liver parenchyma with no steatohepatitis. The is a **liver cell adenoma** with dense lymphplasmacytic aggregates mimicking lymphoma.	Lesion negative, normal liver distribution	Lesion negative	Difficult to assess due to the inflammatory cell aggregate. Appears some reduction of reticulin in the lesional area.	Lesion negative	Dense lymphoid aggregates positive, all lesional and non-lesional hepatocytes negative	Lesion negative
BDD-1	Steatosis involves about 40% liver parenchyma with minimum steatohepatitis. There is a well demarcated lesion with bland cytology **favor liver cell adenoma**.	Lesion negative	Lesion negative	Approximately 75% of lesion showed loss of reticulin Diminished reticulin network.	Lesion negative	Some sinusoidal lymphocytes positive, all lesional and non-lesional hepatocytes negative	Lesion negative

Table S2. Immunohistochemistry characterization of the pMT-N6 cohort samples.

	H&E	Glutamine synthetase	CD34	Reticulin	Beta-catenin	CD44	Glypican 3
N6-12	Dense lymphoplasmacytic aggregates seen in 5 portal tracts. Steatosis involves about 45% liver parenchyma with mild steatohepatitis. **No tumor.**	Normal distribution staining	No tumor	Normal staining pattern	No lesion. Cytoplasmic positivity seen in liver cells at the edge of the tissue (edge effect)	negative	Essentially all negative. At one edge, patch 1-2+ staining noted.
N6-11	Steatosis involves about 40% liver parenchyma with moderate steatohepatitis. Occasional portal tract has dense lymphplasmacytic aggregate. There is one well-defined lesion with 100% steatosis, **favor a small adenoma.**	The nodule showed no staining	Patchy positivity inside nodule	Entire lesion showed diminished staining	Lesion negative. Some inflammatory cells positive.	Lesion negative	Lesion negative
N6-10	Steatosis involves about 35% liver parenchyma with mild steatohepatitis. Occasional portal tract has dense lymphplasmacytic aggregate. There is one well-defined subcapsular lesion with 80% steatosis and mild cytological atypia, **favor liver cell adenoma.**	Tumor mostly positive	Lesion negative	Lesion cells 1-2 cells thick, normal reticulin	Lesion negative	Lesion negative	Lesion negative
N6-9	Steatosis involves about 35% liver parenchyma with mild steatohepatitis. Occasional portal tract has dense lymphplasmacytic aggregate. There is one well-defined lesion with dense cellularity and moderate cytological atypia, **favor early HCC.**	Tumor diffuse strong staining	Lesion negative	Diminished reticulin, thick trabeculae, consistent with HCC	Lesion negative	Lesion negative	The lesion showed diffuse faint positivity 1+, better appreciate at low power
N6-8	Steatosis involves about 45% liver parenchyma with mild steatohepatitis. There are two lesions, one is better demarcated than the other. The well-defined lesion has mild cytological atypia, **favor liver cell adenoma.**	The poorly demarcated nodule, no staining, the well demarcated nodule showed patchy staining	The poorly demarcated nodule, showed some intralesional positivity, the well demarcated nodule is completely negative	The poorly demarcated nodule completely lost reticulin, favor HCC. The well demarcated nodule reticulin diminished.	The poorly demarcated nodule showed areas of nuclear and cytoplasm positivity. The well demarcated nodule mostly negative with some inflammatory cells positive.	Lesion showed focal positivity 2+, mostly inflammatory cells in sinusoids are positive. Only a few hepatocytes positive.	The lesion showed patchy focal positivity 1-2+
N6-7	Steatosis involves about 20% liver parenchyma with mild steatohepatitis. **No tumor.**	Normal distribution staining. At one edge, a poorly demarcated intensive staining area noted.	No tumor.	Normal staining pattern	No tumor. A focal positive are likely due to staining artefact	Some sinusoidal lymphocytes positive, all hepatocytes negative	Patch 1-2+ staining, especially at one edge where the hepatocyte nuclei appears a bit atypical
N6-6	Steatosis involves about 60% liver parenchyma with mild steatohepatitis. Occasional portal tract has dense lymphplasmacytic aggregate. A very small nodular area noted, no obvious cytological atypia. **Could evolve into an adenoma but not there yet.**	Normal distribution staining, a small nodular focus showed lack of staining	A small nodular focus, no stain.	The nodular focus showed slightly diminished reticulin, not obvious	Lesion negative	In addition to the sinusoidal lymphocytes, the lesional hepatocytes showed faint membranous staining 1+	Patchy 1-2+ staining, especially at the nodular focus area.
N6-5	Steatosis involves about 65% liver parenchyma with mild steatohepatitis. There is one well-defined lesion with 75% steatosis, **favor liver cell adenoma.**	Lesion negative	Lesion negative	Reticulin loss in the lesion area	Lesion negative. At the interface with non-neoplastic liver, focal cytoplasmic positivity noted.	Lesion negative	Very small focal areas in the lesion positive (1-2+). Mostly the lesion negative
N6-4	Steatosis involves about 85% liver parenchyma with mild steatohepatitis. There is a 0.07 cm area with cell ballooning and start forming a nodular appearance. **No definitive tumor.**	Normal distribution staining	Negative	Normal reticulin network	No lesion, staining quality not good, cytoplasmic staining see in patchy areas, probably not real.	All negative	Focal and patchy 2+ staining noted.
N6-3	Steatosis involves about 65% liver parenchyma with mild steatohepatitis. **No tumor.**	Normal distribution staining	Negative	Normal reticulin network	No lesion. Cytoplasmic positivity seen in liver cells at the edge of the tissue (edge effect)	All negative	No tumor, all negative
N6-2	Steatosis involves about 10% liver parenchyma with mild steatohepatitis. Occasional portal tract has dense lymphplasmacytic aggregate. There is one well-defined lesion with obvious cytological atypia and mitoses, **favor early evolving hepatocellular carcinoma.** Two small poorly demarcated nodules with similar degree cytological atypia can also be appreciated.	Showed 3 nodules, all positive	Lesions all Negative. Only one nodule obvious	Reticulin loss in noe nodule. Diminished reticulin in two other nodules.	2 small lesions negative. 1 larger lesion showed focal patchy cytoplasmic positivity	one small lesion negative. The larger well recognized lesion and one small lesion showed 1+ membranous staining on hepatocytes	2 small lesions negative. The larger well recognized lesion positive (1-2+)
N6-1	Steatosis involves about 35% liver parenchyma with mild steatohepatitis. Occasional portal tract has dense lymphplasmacytic aggregate. There is one well-defined lesion **well differentiated hepatocellular carcinoma.** Two small poorly demarcated nodules with similar degree cytological atypia can also be appreciated.	Tumor diffusely positive	Strong positivity inside the tumor in two lesions. 3rd one no stain (unable to recognize the nodule)	The large nodule showed areas lost reticulin. Favor malignant.	Lesion strong cytoplasmic positivity, patchy but real	Tumor negative. The dense lymphoid aggregate between two vessels showed 3+ staining.	Entire lesion faint positive 1+. Non-neoplastic liver showed patchy positivity (2+).

Table S3. Immunohistochemistry scores of tumor markers in the BDD and N6 cohort samples.

Scoring Interpretation- *Reticulin*: Reticulin lost is suggestive of malignancy.[9,10] The progressive lost of associated reticulin fiber is labeled as follows: 3+: Intact reticulin pattern (1-2 cells thickening of hepatic plates), 2+: Weak (2-3 cells thickening of hepatic plates), 1+: Moderate (>4 cells thickening of hepatic plates), and Neg: Complete loss of the reticulin. ***Glypican-3:*** Cytoplasmic granular staining supports malignancy.[10,14,15] Presence of cytoplasmic diffused or patchy and/or focal patterns are labeled with different intensity as follows: 3+: Strong positivity, 2+: Moderate positivity, 1+: Weak positivity, and Neg: No Positive staining. ***CD34:*** Diffused and strong sinusoidal endothelial cell staining is observed in almost all HCC cases.[10,12] The endothelial cells of the sinusoidal wall are labeled as follows: 2+: Diffusely Positive (>80% endothelial cells of the sinusoidal wall), 1+: Focally Positive (30-80% endothelial cells of the sinusoidal wall), and Neg: Negative (<30% endothelial cells of the sinusoidal wall). ***Glutamine Synthetase:*** HCCs tumors show strong positive staining while adenomas may occasionally show positive staining.[14,19,20] Lesions are labeled as follows: Pos. Diffused: Diffused cytoplasmic positivity, Pos. Patchy: Patch like cytoplasmic positivity, Pos. Weak: Weak cytoplasmic positivity, and Neg: No positive staining. In normal liver, glutamine synthetase is confined in 2-3 cell-thick hepatocytes around the central vein and is labeled as: Pos. CV. ***β -Catenin:*** Nuclear accumulation of β-catenin is suggestive of malignant transformation.[21,22] Presence of cytoplasmic and/or nuclear staining in cancer cells are labeled as follows: Diffused: Diffused cytoplasmic Positivity, Nuclear: Nuclear positive staining, Diffused & Nuclear: Diffused cytoplasmic and nuclear positivity, and Neg: No Positive staining. ***CD44:*** Upregulation of CD44 expression is associated with HCC development.[28,29] Diffused or focal staining patterns of CD44 in cancer cells or hepatocytes is labeled as follows: 3+: Strong membranous positive cells, 2+: Moderate membranous positive cells, 1+: Weak membranous positive cells, and Neg: No positive staining.

Liver Samples	# of Tumors	Lesions Type	Reticulin	Glypican-3	CD34	Glutamine Synthetase	β-catenin	CD44
BBD-1	1	Adenoma	2+	Neg	Neg	Neg	Neg	Neg
BBD-2	1	Adenoma	3+	Neg	Neg	Neg	Neg	Neg
BBD-3	1	HCC	Neg	Neg	2+	Neg	Cytoplasmic	Neg
BBD-4	1	Adenoma	2+	Neg	Neg	Neg	Neg	Neg
BBD-5	1	Adenoma	2+	Neg	Neg	Pos, Patchy	Neg	Focal, 1+
BBD-6	1	Adenoma	3+	Neg	Neg	Neg	Neg	Neg
BBD-7	1	HCC	1+	Neg	1+	Neg	Neg	Neg
BBD-8	1	HCC	1+	Patchy, 1+	2+	Pos, Diffused	Nuclear	Neg
BBD-9	1	HCC	Neg	Focal, 1+	Neg	Pos, Diffused	Neg	Neg
BBD-10	1	Adenoma	2+	Neg	1+	Neg	Cytoplasmic & Nuclear	Neg
N6-1	3	HCC	Neg	Diffused, 2+	2+	Pos, Diffused	Cytoplasmic	Neg
N6-2	3	HCC	2+	Diffused, 1-2+	2+	Pos, Diffused	Cytoplasmic	Focal, 1+
N6-3	0	N/A	3+	Neg	Neg	Pos, CV	Neg	Neg
N6-4	0	N/A	3+	Patchy & Focal, 2+	Neg	Pos, CV	Neg	Neg
N6-5	1	Adenoma	2+	Neg	Neg	Neg	Cytoplasmic	Neg
N6-6	0	N/A	3+	Patchy, 1-2+	Neg	Pos, CV	Neg	Weak, 1+
N6-7	0	N/A	3+	Patchy, 1-2+	Neg	Pos, CV	Neg	Neg
N6-8	2	Adenoma	2+	Patchy & Focal, 1-2+	Neg	Pos, Patchy	Neg	Focal, 2+
N6-9	1	HCC	Neg	Diffused, 1+	Neg	Pos, Diffused	Neg	Neg
N6-10	1	Adenoma	3+	Neg	Neg	Pos, Diffused	Neg	Neg
N6-11	1	Adenoma	2+	Neg	1+	Neg	Neg	Neg
N6-12	0	N/A	3+	Neg	Neg	Pos, CV	Neg	Neg

Table S4. BDD and N6 DNA in tumor and non-tumor tissues in livers of cohorts of pMT-BDD and pMT-N6 injected mice was not detectable by quantitative PCR analysis. DNAs were isolated from the tumor and non-tumor tissues of FFPE liver blocks of mice listed below and subjected to qPCR analysis as described in Methods, with mouse beta actin (*Actb*) as an internal control samples to normalize the data for BDD and N6 vector sequence detection [F8/*Actb*= 2^(Cq-*Actb* – Cq-F8)]. Except for the positive control DNA (*i,e*., pMT-BDD at 24h) sample (F8/*Actb* = 11.17), the F8/*Actb* values for all other samples were within the range of background noise, indicating the absence of the BDD or N6 sequence. NA: non-applicable; ND: not determined due to insufficient amounts of tissues; NV: no value /below detection limit.

		Quantification cycle (Cq)					
		Tumor			Non-tumor		
	Sample ID	F8	*Actb*	F8/*Actb*	F8	*Actb*	F8/*Actb*
Negative control	Saline-24h	NA	NA	NA	27.004	21.427	0.021
Positive control	pMT-BDD-24h	NA	NA	NA	17.771	21.253	11.169
pMT-BDD cohort	BDD-1	35.745	27.175	0.003	33.470	26.950	0.011
	BDD-2	NV	30.958	NV	34.244	31.244	0.125
	BDD-3	NV	25.997	NV	NV	26.540	NV
	BDD-4	NV	30.634	NV	38.436	31.159	0.006
	BDD-5	37.637	27.746	0.001	NV	28.466	NV
	BDD-6	33.283	27.094	0.014	35.302	25.668	0.001
	BDD-7	ND	ND	ND	34.860	26.278	0.003
	BDD-8	33.836	26.908	0.008	ND	ND	ND
	BDD-9	34.006	26.091	0.004	35.160	27.183	0.004
	BDD-10	33.373	29.238	0.057	34.749	30.486	0.052
pMT-N6 cohort	N6-1	35.274	28.220	0.008	35.665	26.535	0.002
	N6-2	33.325	29.441	0.068	NV	32.852	NV
	N6-3	NA	NA	NA	34.267	29.593	0.039
	N6-4	NA	NA	NA	36.750	26.847	0.001
	N6-5	38.596	34.724	0.068	NV	28.666	NV
	N6-6	NA	NA	NA	NV	29.190	NV
	N6-7	NA	NA	NA	34.546	27.072	0.006
	N6-8	37.233	29.000	0.003	36.919	27.365	0.001
	N6-9	36.809	28.160	0.002	36.084	30.111	0.016
	N6-10	34.615	26.158	0.003	34.491	26.627	0.004
	N6-11	NV	NV	NV	34.421	26.518	0.004
	N6-12	NA	NA	NA	33.894	29.693	0.054